environmental microbiology

Environmental Microbiology (2022) **24**(6), 2732–2746 doi:10.1111/1462-2920.15888

Special Issue Article

Nod factor-independent 'crack-entry' symbiosis in dalbergoid legume *Arachis hypogaea*

Sohini Guha,[1*] Firoz Molla,[1] Monolina Sarkar,[1] Fernando Ibañez,[2] Adriana Fabra[2] and Maitrayee DasGupta[1*]

[1]*Department of Biochemistry, University of Calcutta, Kolkata, 700019, India.*

[2]*Instituto de Investigaciones Agrobiotecnologicas (CONCINET-UNRC), Ruta 36 Km 601, Río Cuarto, Argentina.*

Summary

Dalbergoids are typified by crack-entry symbiosis which is evidenced to be Nod Factor (NF)-independent in several *Aeschynomene* legumes. Natural symbionts of the dalbergoid legume *Arachis hypogaea* are always NF-producing, prompting us to check whether symbiosis in this legume could also be NF-independent. For this, we followed the symbiosis with two NF-containing bradyrhizobial strains – SEMIA6144, a natural symbiont of *Arachis* and ORS285, a versatile nodulator of *Aeschynomene* legumes, along with their corresponding nodulation (*nod*) mutants. Additionally, we investigated NF-deficient bradyrhizobia like BTAi1, a natural symbiont of *Aeschynomene indica* and the WBOS strains that were natural endophytes of *Oryza sativa*, collected from an *Arachis-Oryza* intercropped field. While SEMIA6144ΔnodC was non-nodulating, both ORS285 and ORS285ΔnodB could induce functional nodulation, although with lower efficiency than SEMIA6144. On the other hand, all the NF-deficient strains – BTAi1, WBOS2 and WBOS4 showed comparable nodulation with ORS285 indicating *Arachis* to harbour an NF-independent mechanism of symbiosis. Intriguingly, symbiosis in *Arachis*, irrespective of whether it was NF-dependent or independent, was always associated with the curling or branching of the rosette root hairs at the lateral root bases. Thus, despite being predominantly described as an NF-dependent legume, *Arachis* does retain a vestigial, less-efficient form of NF-independent symbiosis.

Received 8 October, 2021; revised 9 December, 2021; accepted 21 December, 2021. *For correspondence. Tel. 033-2461-4714; Fax 91-33-2461-4849; E-mail 2019guhasohini@gmail.com. maitrayee_d@hotmail.com.

Introduction

Root nodule symbiosis (RNS) within legumes leads to the formation of nodules which house diazotrophs called rhizobia responsible for nitrogen fixation (Oldroyd, 2013). RNS consists of two main developmental pathways – rhizobial invasion and nodule organogenesis (Oldroyd *et al*., 2011). The most common mode of rhizobial invasion happens via 'root hair entry' through intracellular infection threads (IT) which is encountered within legumes like *Medicago* spp., *Glycine max* (*G. max*), *Lotus japonicus* (*L. japonicus*) (Oldroyd *et al*., 2011; Okazaki *et al*., 2013). A slight variation to this mode of entry is seen within legumes like *Sesbania rostrata* (*S. rostrata*) and *Neptunia* where the rhizobia enter via epidermal cracks followed by the formation of transcellular IT (Goormachtig *et al*., 2004). Contrary to these, 25% of legumes, mostly plants of the subtropical genera *Aeschynomene*, *Stylosanthes* and *Arachis* are supported by a simpler mode of rhizobial invasion called 'crack-entry' where the bacteria enter the plant via epidermal cracks at the lateral root bases (LRBs), in an intercellular manner, without the formation of any IT (Sprent, 2007). These diverse modes of rhizobial invasion are governed by either of the two underlying mechanisms of symbiosis, NF-dependent or NF-independent (Madsen *et al*., 2010). During NF-dependent symbiosis, initiation of RNS involves perception of the plant flavonoids by the incoming rhizobia which in turn secrete specialized lipochitooligosaccharides called the Nod Factors (NFs) (Oldroyd *et al*., 2011). These NFs are recognized by certain legume receptor kinases known as the Nod-Factor receptors which signal a downstream 'Sym Pathway' that causes the root hair curling (RHC) and IT formation which eventually results in RNS (Oldroyd *et al*., 2011; Oldroyd, 2013). This NF-dependent mechanism of symbiosis is functional within both IT as well non-IT legumes and was considered the sole pathway for establishment of RNS. However, with

the discovery of a set of bradyrhizobia lacking the canonical nodulation (*nodABC*) genes responsible for the production of NFs, the existence of the NF-independent mechanism came to light. Certain legumes of the *Aeschynomene* genus are evidenced to undertake RNS with these NF-deficient bradyrhizobia (Giraud *et al*., 2007).

The genus *Aeschynomene* exhibits intrageneric diversity in terms of the mechanism of symbiosis adapted by them. Classified into three cross-inoculation (CI) groups according to their associated microbes, members of CI-I and CI-II groups and their cognate bradyrhizobia like *Aeschynomene americana–Bradyrhizobium* sp. DOA9 (CI-I) and *Aeschynomene afraspera–Bradyrhizobium* sp. ORS285 (CI-II) use the NF-dependent mechanism of symbiosis for RNS (Chaintreuil *et al*., 2013). However, the CI-III group which includes *Aeschynomene indica* (*A. indica*) and its diploid progenitor *Aeschynomene evenia* (*A. evenia*) nodulates with NF-deficient *Bradyrhizobium* sp. BTAi1 or with NF containing ORS285 in an NF-independent manner (Miche *et al*., 2010; Arrighi *et al*., 2012; Okubo *et al*., 2012).

Arachis is a 'crack-entry' legume which is phylogenetically close to the *Aeschynomene* genus (Lavin *et al*., 2001). Despite having physical resemblance in their patterns of colonization, under field conditions, *Arachis* is preferentially colonized by *nod* containing *Bradyrhizobium* (Guha *et al*., 2016). With the cognate strain *Bradyrhizobium* sp. SEMIA6144, it undertakes nodulation using the NF-dependent mechanism (Ibáñez and Fabra, 2011). However, under controlled conditions, this legume is evidenced to induce suboptimal yet persistent functional nodulation with NF-deficient strains like BTAi1 (Noisangiam *et al*., 2012). Additionally, bradyrhizobial WBOS strains that were isolated as endophytes from *Oryza* and were demonstrated to be *nod* deficient by both PCR and Southern Hybridisation experiments could also induce functional nodulation in *Arachis*, raising the possibility of the existence of an NF-independent mechanism (Guha *et al*., 2016). Nevertheless, these observations were performed with unlabelled strains, raising the question of nodulation by potential NF-producing rhizobia. In this study, a labelled collection of *Bradyrhizobium* strains comprising of SEMIA6144, ORS285, their corresponding *nod* mutants and some natural NF-deficient strains were used to demonstrate the existence of NF-independent symbiosis within *Arachis*.

Results

Selection of bradyrhizobial strains for studying NF-independent symbiosis in Arachis *and their Tn7-based labelling*

To undertake a systematic investigation for demonstrating an NF-independent nodulation within *Arachis*, our first objective was to develop fluorescently labelled bradyrhizobial strains. For this, we checked the nodulation efficiencies of two NF containing strains – SEMIA6144, a natural symbiont of *Arachis* and ORS285, a versatile nodulator of *Aeschynomene* legumes, along with their corresponding *nod* mutants across four *Arachis* cultivars (Fig. 1). Unlike ORS285, which showed cultivar specificity, SEMIA6144 was a robust nodulator across all the four cultivars. Both ORS285 and ORS285ΔnodB were able to develop functional nodules in *Arachis* cv. JL501, whereas SEMIA6144ΔnodC was non-nodulating in all the four cultivars. Additionally, we chose to investigate NF-deficient strains like BTAi1, a natural symbiont of *A. indica*, and the strains from the WBOS series that were natural endophytes of *Oryza*, collected from an *Arachis-Oryza* intercropped field. BTAi1 could nodulate all the four cultivars of *Arachis* but WBOS strains could be classified into cultivar-specific and cultivar-independent nodulators (Fig. 1). We selected three WBOS strains from each of these two categories for further investigation. Since all the selected strains were sensitive to spectinomycin (Table S1), we used pUC18-mini-Tn7T-aad9 for designing the fluorescent tag bearing plasmids (Lehman *et al*., 2016) (Table S2). Tn7 transposition occurs downstream to the *glmS* gene which encodes Glucosamine-6-phosphate synthetase (Choi *et al*., 2005) (Fig. S1A). To confirm Tn7 insertion, PCR was performed, using primer pairs glmS-$_{down}$/aad9-$_{rev}$, spanning the 3′ end of *glmS*, and the 3′ end of the *aad9* gene encoding spectinomycin cassette whereby a band of approximately 1.5 kb size was amplified from the labelled strains (Fig. S1B). Subsequent sequencing of the amplicons revealed the Tn7 cluster to be inserted 25 base pairs downstream to the *glmS* in all the labelled strains, which matched earlier reports (Choi *et al*., 2005) (Fig. S1C). The strains maintained their fluorescence under free-living conditions, even in the absence of antibiotics (Fig. S1D).

Aeschynomene indica*, a strictly NF-independent nodulator is successfully nodulated by WBOS strains*

While the NF-independent nodulation in *A. indica* is well established with BTAi1, ORS285 and its *nod* mutant, the symbiotic behaviour of the WBOS strains remain untested. So our next objective was to check whether the WBOS strains could support nodulation in an established NF-independent legume, *A. indica*. A total of 50 plants per strain were harvested at 30 dpi and checked for nodulation, plant growth promotion and nitrogen fixation. All nodules produced on *A. indica* during the nodulation assays were either GFP or mCherry labelled, depending on the strains used. The frequency of *A. indica* plants nodulated by WBOS strains was irregular and low in comparison to BTAi1, ORS285 and ORS285ΔnodB (Fig. 2A; Table S3). Among the selected WBOS strains,

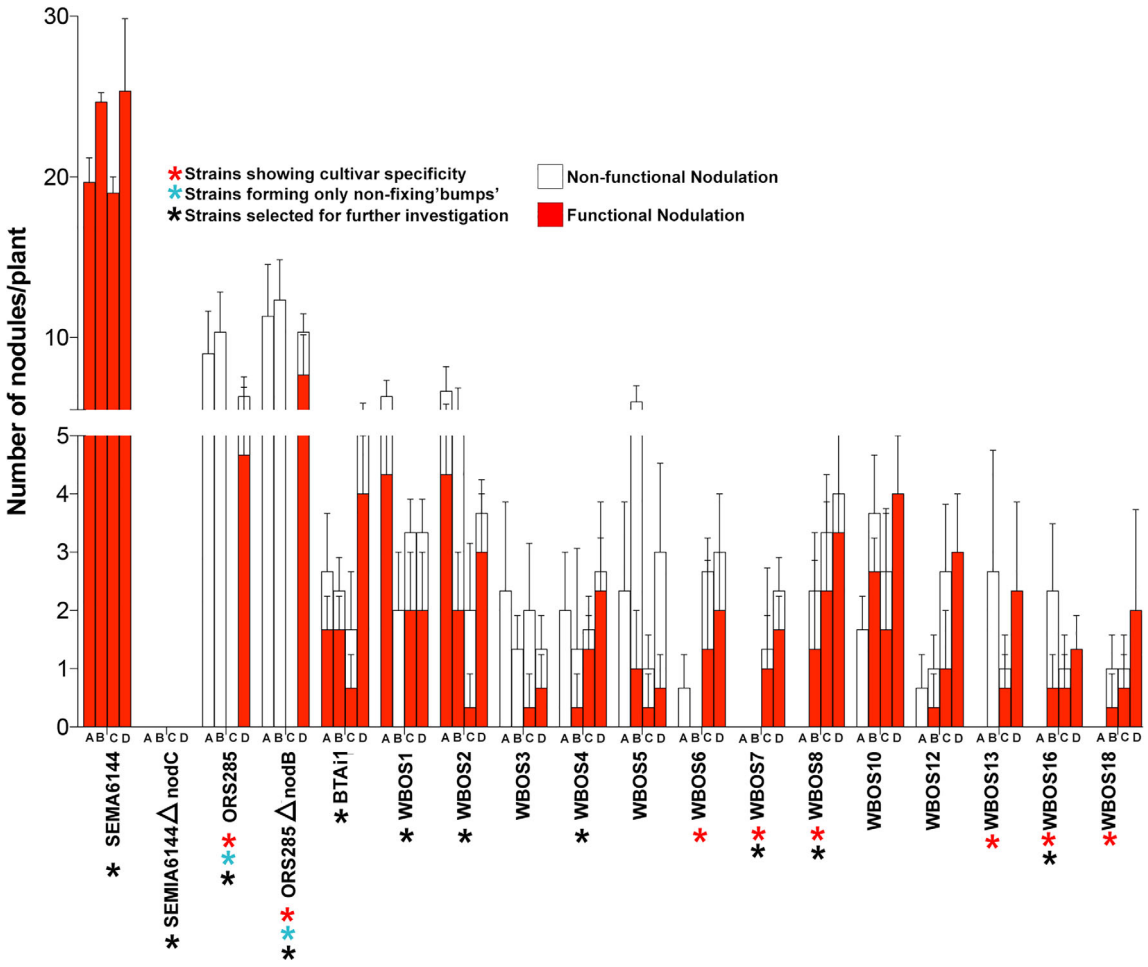

Fig. 1. Comparative nodulation behaviour of selected *Bradyrhizobium* across four *Arachis* cultivars. The four *Arachis* cultivars are represented by – JL24 (A), Lal badam (B), ICGV9114 (C), and JL501 (D). Solid bars represent the number of functional nodules produced by the indicated strains, whereas hollow bars represent non-functional nodulation by the same. Strains marked in red asterisks exhibit cultivar specificity. Strains marked in cyan asterisks induced non-functional nodules in the form of uncolonized 'bumps', whereas the rest of the strains having hollow bars produced non-fixing white nodules. Strains marked in black asterisks were selected for further experiment. The number of plants per strain (*n*) was 20.

WBOS1, WBOS2 and WBOS8 could nodulate *A. indica* and WBOS4, WBOS7 and WBOS16 failed to nodulate but could successfully colonize the LRBs (Fig. 2B and E; Table S3). While all BTAi1, ORS285 and ORS285ΔnodB infected plants nodulated (~10–16 nodules/plant), only ~40%–50% of the plants induced functional nodules in presence of WBOS1 and WBOS2 (~4 nodules/plant). Intriguingly, in spite of low nodulation there was a considerable increase in biomass in WBOS1 and WBOS2 infected plants compared to the optimal symbionts BTAi1 or ORS285. (Fig. 2A, C, D; Fig. S2; Table S3). Ultrastructures of the fluorescent nodules induced by both WBOS1 and WBOS2 had typical aeschynomenoid infection zones which upon magnification revealed spherical bacteroids identical to those produced by BTAi1, ORS285 and ORS285ΔnodB (Fig. 2E and F). Compared to WBOS1 and WBOS2, nodulation was insignificant with WBOS8 (~1 nodule/plant) where the developed nodules were always non-fixing with undifferentiated rod-shaped rhizobia (Fig. 2B, D, F; Table S3). Similar to WBOS8, the NF containing SEMIA6144 and its *nodC* mutant also showed insignificant nodulation in *A. indica* (~1 nodule/plant) with only 4%–10% of the plants nodulating and the nodules formed were always non-functional (Fig. 2B, D, F; Table S3). It may be noted that in spite of insignificant nodulation with WBOS8, SEMIA6144 and SEMIA6144ΔnodC, we consistently observed some increase in biomass among the nodulated plants without any signs of nitrogen starvation (Fig. 2C; Fig. S2; Table S3). Taken together, although *Arachis* and *Aeschynomene* are phylogenetically close crack-entry legumes, we find that the WBOS strains which were nodulating in *Arachis* may not nodulate *A. indica*. Our results indicate that WBOS1 and WBOS2 have the

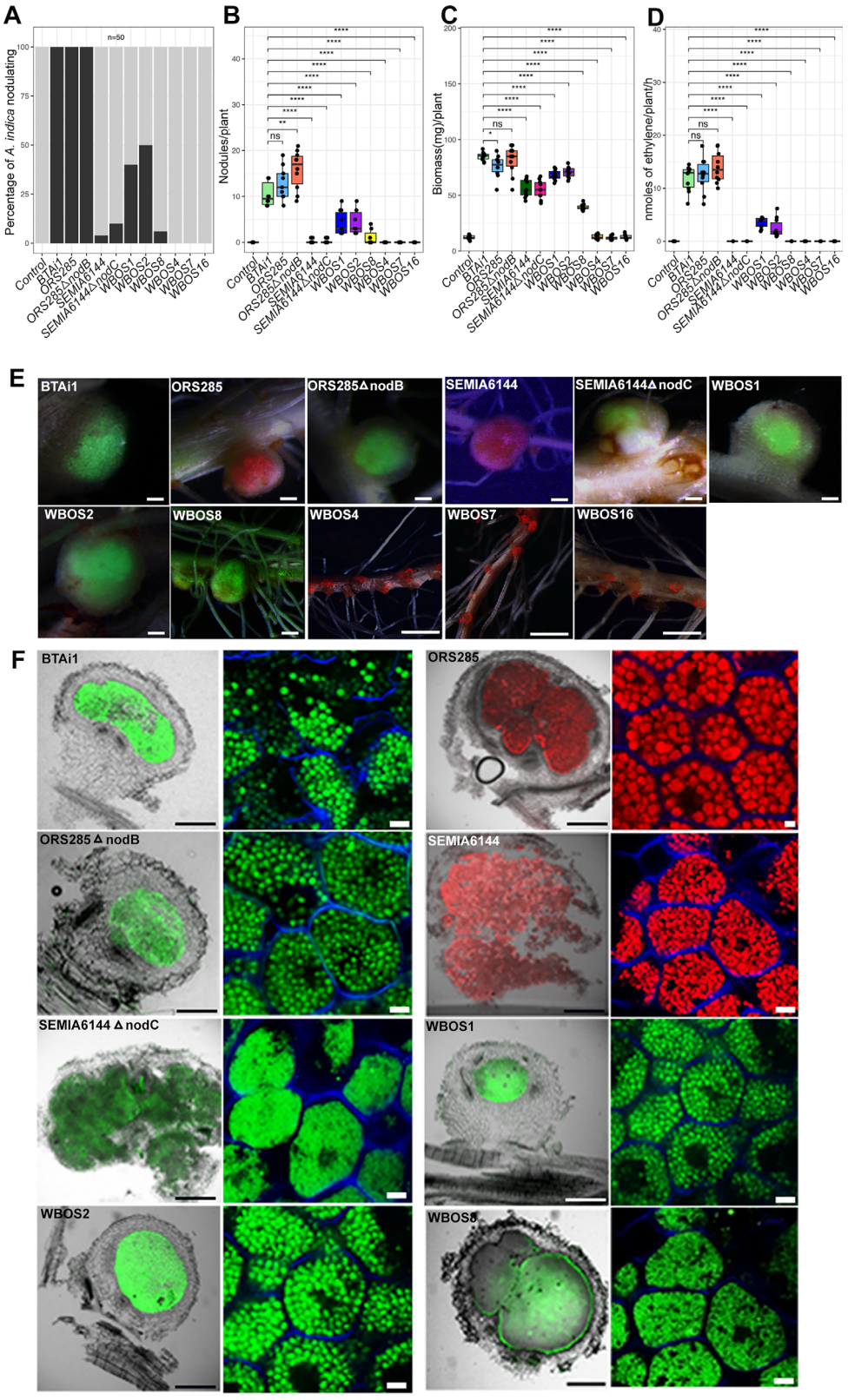

Fig. 2. Legend on next page.

required tools for the inception of functional NF-independent symbiosis, specifically adapted in *A. indica*.

Arachis *can undertake NF-independent symbiosis*

For an in-depth analysis of NF-independent symbiosis within *Arachis*, we monitored nodulation in presence of SEMIA6144, SEMIA6144ΔnodC, ORS285, ORS285ΔnodB and NF-deficient strain BTAi1 in the cultivar JL501. Among the WBOS strains, we chose WBOS2, which could nodulate *A. indica* and WBOS4 which despite being NF-deficient did not nodulate *A. indica*. A total of 100 plants per strain were harvested at 30 dpi and checked for nodulation, plant growth promotion and nitrogen fixation. All the nodules produced in *Arachis* during the nodulation assays were either GFP or mCherry labelled depending on the strain used (Fig. S3.). When the NF-cassette was disrupted in SEMIA6144, it failed to nodulate *Arachis*, whereas contrary to this, disruption of NF-cassette in ORS285 did not affect the ability of the strain to nodulate (Fig. 3A). This indicates ORS285 to undertake an NF-independent symbiosis in *Arachis*, which is similar to its symbiotic behaviour demonstrated in *A. indica* (Bonaldi *et al*., 2011). In fact, the frequency of nodulation of NF-deficient strains – BTAi1, WBOS2 and WBOS4 in *Arachis* was lower than SEMIA6144 but was comparable with ORS285 and ORS285ΔnodB (Fig. 3A; Table S4). While all the SEMIA6144 inoculated plants registered nodulation (~25 nodules/plant), only 10%–25% of the plants were nodulated with ORS285, ORS285ΔnodB and the NF-deficient strains (~3–5 nodules/plant) (Fig. 3A and B; Table S4). Irrespective of the stark difference in nodulation frequency, all the strains with the exception of SEMIA6144ΔnodC showed a consistent increase in biomass, almost similar to SEMIA6144 (Fig. 3C; Fig. S4; Table S4). The growth promotion effects of WBOS strains on *Arachis* has been reported earlier (Guha *et al*., 2016), and it was interesting to observe that BTAi1 induced similar growth promotion, despite being a weak nodulator. The plant growth promotion of the strains might result from a number of factors other than nitrogen fixation, particularly, siderophore production which is evidenced to increase the nitrogen content of legume shoots (Jaiswal *et al*., 2021). The nodules induced by all the NF-deficient strains had a red interior which is related to the presence of leghaemoglobin and is an indicator of an effective nodule nitrogen fixation activity. In addition, positive response in acetylene reduction assays further confirmed these nodules to be functional (Fig. 3D and E; Table S4). The nitrogen fixation abilities of the NF-deficient strains were significantly less compared to SEMIA6144 but intriguingly the fixation ability of both ORS285 and ORS285ΔnodB was significantly higher than the NF-deficient strains (*P*-value = <0.0001) (Fig. 3D; Table S4). In accordance with the functional nodules developed with the strains, the ultrastructural analysis revealed all the strains to mature into well-differentiated spherical bacteroids identical to SEMIA6144 (Fig. 3F). Additionally, the fact that WBOS2 and WBOS4 strains differentially nodulated *A. indica*, but induced comparable nodulation in *Arachis*, indicates the diversities of NF-independent mechanisms.

Finally, SEMIA6144ΔnodC failed to nodulate *Arachis*, indicating that the mere absence of NFs does not ensure symbiosis in *Arachis* but requires some other dependencies such as that present in ORS285 as well as in the NF-deficient strains.

Both NF-producing and NF-deficient Bradyrhizobium *induce RHC in* Arachis

Aeschynomene legumes have characteristic axillary root hairs at their LRBs which are commonly referred to as rosette root hairs in *Arachis* (Sinharoy *et al*., 2009; Bonaldi *et al*., 2011). While RHC is not reported within the NF-dependent or independent *Aeschynomene* legumes (Bonaldi *et al*., 2011; Noisangiam *et al*., 2012), an earlier report indicated RHC in *Arachis* (Chandler, 1978). So, we next monitored two traits in *Arachis*: bradyrhizobial colonization at the LRBs and RHC. The efficiencies of both the traits were determined

Fig. 2. Nodulation in *Aeschynomene indica* by selected *Bradyrhizobium* strains.
A. Percentage incidence of nodulation within *A. indica* by selected *Bradyrhizobium* strains. The black and grey areas per bar represent the percentage of nodulated and non-nodulated plants respectively, infected with the indicated *Bradyrhizobium* where number of plants per strain (*n*) was 50. For all nodulating strains, only nodulated plants were used for quantification of nodules/plant, plant dry weight and acetylene reduction assay.
B. The number of nodules per plant.
C. Plant growth promotion.
D. nmoles of ethylene produced by the plants per hour infected with the indicated strains. For (B–D), each data point represents one independent replicate and each experiment involved 10 plants per strain. One-way ANOVA was used to assess the significant differences among the groups with *P*-values adjusted by Tukey's Multiple Comparison Test. Comparisons with positive control strain BTAi1 indicated. $P > 0.05$ is considered not significant (n.s.), whereas '*', '**','***' and '****' indicate $P \leq 0.05$, $P \leq 0.01$, $P \leq 0.001$ and $P \leq 0.0001$ respectively.
E. Stereomicroscope images of fluorescent nodules and colonized roots induced in *A. indica* by indicated strains. Nodules are represented as merged images of bright-field + GFP/mCherry. Scale bar: 500 μm (for *A. indica* nodules); 2 mm (for *A. indica* roots).
F. Microscopy of the whole nodule sections, induced by the indicated strains (left) and corresponding enlarged view of the infection centres (right). Scale bars for whole nodule sections – 200 μm; for enlarged view of the infection centres – 20 μm (ORS285), rest – 40 μm .

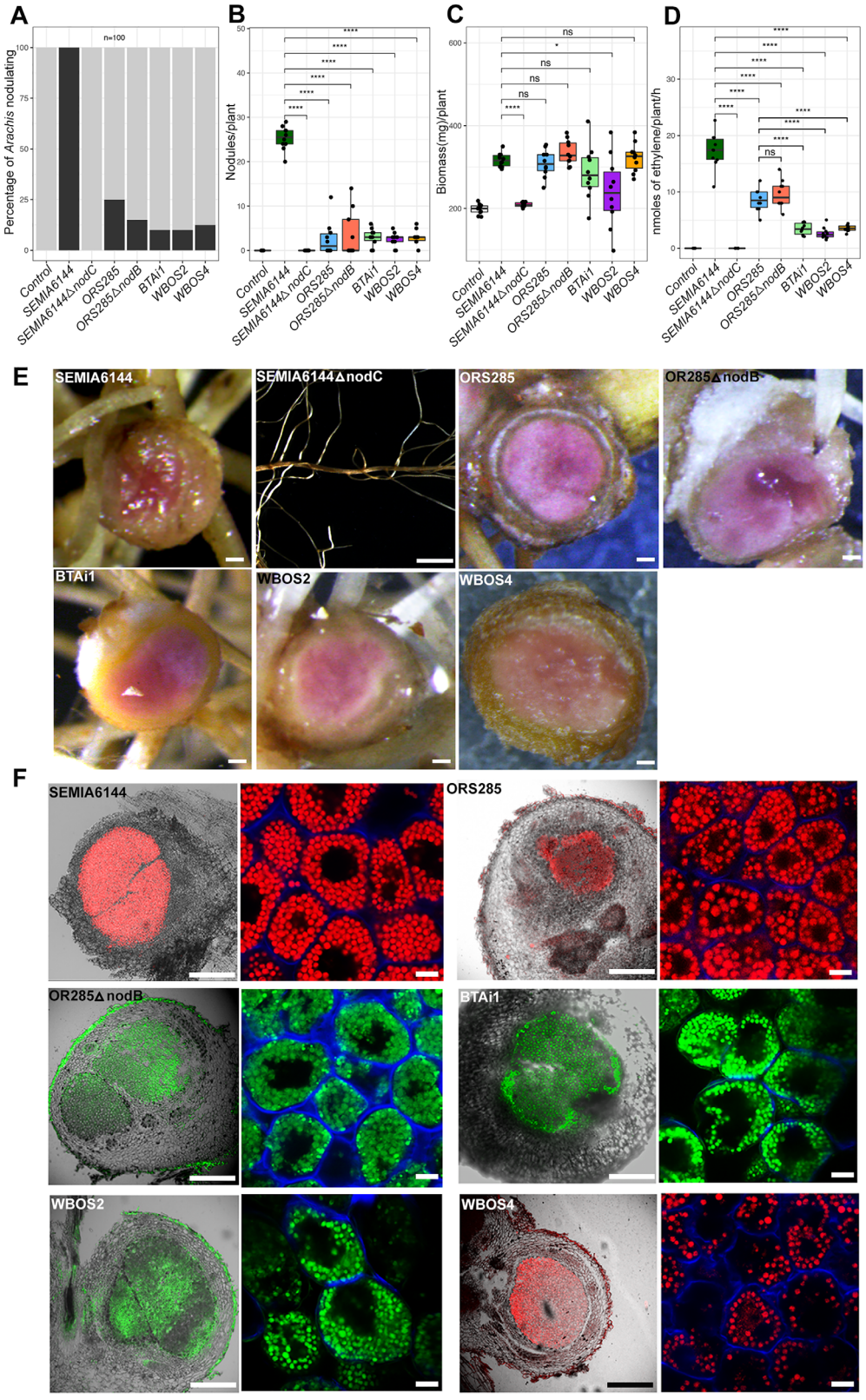

Fig. 3. Legend on next page.

by calculating the number of LRBs/plant colonized by the strains and the number of RHCs/LRB respectively. All the tested strains colonized the LRBs of infected plants as annular fluorescent rings, indicating that the colonization of these strains was independent of NFs. While all the plants infected with SEMIA6144 and SEMIA6144ΔnodC were colonized (~11–15 LRBs/plant), only 40%–60% of the plants were colonized by ORS285, its *nodB* mutant and the NF-deficient strains (~1–5 LRBs/plant) (Fig. 4A and C; Table S5). SEMIA6144ΔnodC additionally appeared to form a biofilm in the vicinity of the LRBs, something that we occasionally noticed also with BTAi1 and WBOS2 (Fig. 4E). Intriguingly, symbiosis in *Arachis*, irrespective of whether it was NF-dependent or independent, was always associated with the curling or branching of the rosette root hairs at the LRB. Except for SEMIA6144ΔnodC, which failed to induce any nodulation in *Arachis*, all the tested strains were found to induce root hair branching and RHC (Fig. S5 and Fig. 4B and E). Thus, both an NF-dependent and an independent mechanism can induce RHC in *Arachis*. While SEMIA6144 infected plants developed ~15 RHCs/LRB, ORS285 and ORS285ΔnodB developed ~4 RHCs/LRB and for the NF-deficient strains, only ~1–2 RHCs/LRB was noted, indicating the NF-independent trigger to be less potent (Fig. 4D and E; Table S5). In addition to RHC, entrapment of rhizobia was occasionally noticed only with SEMIA6144 and ORS285 but never with ORS285ΔnodB or the NF-deficient strains (Fig. S6 and Fig. 4E).

Competition between SEMIA6144 and the NF-deficient strains

Competition assays are relevant as they closely resemble in-field realistic scenarios where *Arachis* face a multitude of strains having different dependencies (like presence of *nod* and absence of *nod* genes) and the cumulative symbiotic outcome is a result of the competitive interactions between them (Guha *et al*., 2016). Binary competitions were set between SEMIA6144 and the NF-deficient strains BTAi1, WBOS2 and WBOS4. A total of 10 plants per competition category were harvested at 30 dpi and the nodules were classified as single infected or mixed, based on the emitted fluorescence and subsequent isolation and identification of the colonized rhizobia. The outcome of the competition experiments was widely different, highlighting the complexity of interactions between *Arachis* and its rhizobial symbionts. While co-infection with BTAi1 and with WBOS4 did not affect the nodule numbers compared to SEMIA6144 single strain infected plants (~22–29 nodules/plants), co-infection with WBOS2 significantly repressed the overall nodule count (~13 nodules/plant) (Fig. 5B; Table S6). In all the mixed inoculation experiments, singly occupied and mixed nodules were found among all the experimental plants (Fig. 5A and C; Table S7). In WBOS2-SEMIA6144 co-inoculation experiments, only 11% nodules were singly occupied by SEMIA6144, whereas 55% was occupied by WBOS2 and the rest were mixed nodules (Fig. 5C; Fig. S7; Table S7). Interestingly, during single infection, WBOS2 could only make ~2–3 nodules/plant compared to ~7 nodules/plant in all the WBOS2-SEMIA6144 co-inoculated plants (See Fig. 3B; Table S4). On the other hand, in case of BTAi1-SEMIA6144 co-inoculation, almost ~58% nodules were occupied exclusively by SEMIA6144 compared to ~11% by BTAi1 only and in case of WBOS4-SEMIA6144, ~37% nodules were singly occupied with SEMIA6144 while the rest were mixed (Fig. 5C; Fig. S7; Table S7). Microscopy analyses revealed all singly occupied nodules in these co-inoculation experiments to resemble the nodules developed during single strain inoculation experiments, with properly developed spherical bacteroids (Fig. 5D). But in all cases of dually occupied nodules, microscopy analyses revealed that only SEMIA6144 differentiated into spherical symbiosomes (Fig. 5D). The NF-deficient rhizobia, however, remained rod-shaped within the intercellular spaces, indicating that they were sanctioned against being endocytosed. In rare cases, BTAi1 formed functional spherical symbiosomes along with SEMIA6144 in the same nodule but in distinct zones (Fig. S8). On the other hand, WBOS4

Fig. 3. Nodulation in *Arachis* by selected *Bradyrhizobium* strains.
A. Percentage incidence of nodulation among *Arachis* by the selected *Bradyrhizobium* strains. The black and grey areas per bar represent the percentage of nodulated and non-nodulated plants respectively, infected with the indicated *Bradyrhizobium* where number of plants per strain (*n*) was 100. For all nodulating strains, only nodulated plants were used for quantification of nodules/plant, plant dry weight and acetylene reduction assay.
B. Number of nodules per plant.
C. Plant growth promotion induced by the strains.
D. nmoles of ethylene produced by the plants infected with the indicated strains. (B–D) Each data point represents one independent replicate and each experiment involved 10 replicates per strain. One-way ANOVA was used to assess the significant differences among the groups with *P*-values adjusted by Tukey's Multiple Comparison Test. $P > 0.05$ is considered not significant (n.s.), whereas '*', '**','***' and '****' indicate $P \leq 0.05$, $P \leq 0.01$, $P \leq 0.001$ and $P \leq 0.0001$ respectively.
E. Nodule half sections and non-nodulated roots by indicated strains (Scale bar for nodule half-sections – 500 μm; for non-nodulated root – 2 mm).
F. Fluorescent images of whole nodule sections induced by the indicated strains are represented as bright-field + mCherry or GFP merged images while the corresponding enlarged views of the infection centres are shown as mCherry or GFP and Calcofluor merged images. Scale bars: For whole nodule sections – 200 μm, for enlarged view of the infection centres – 40 μm .

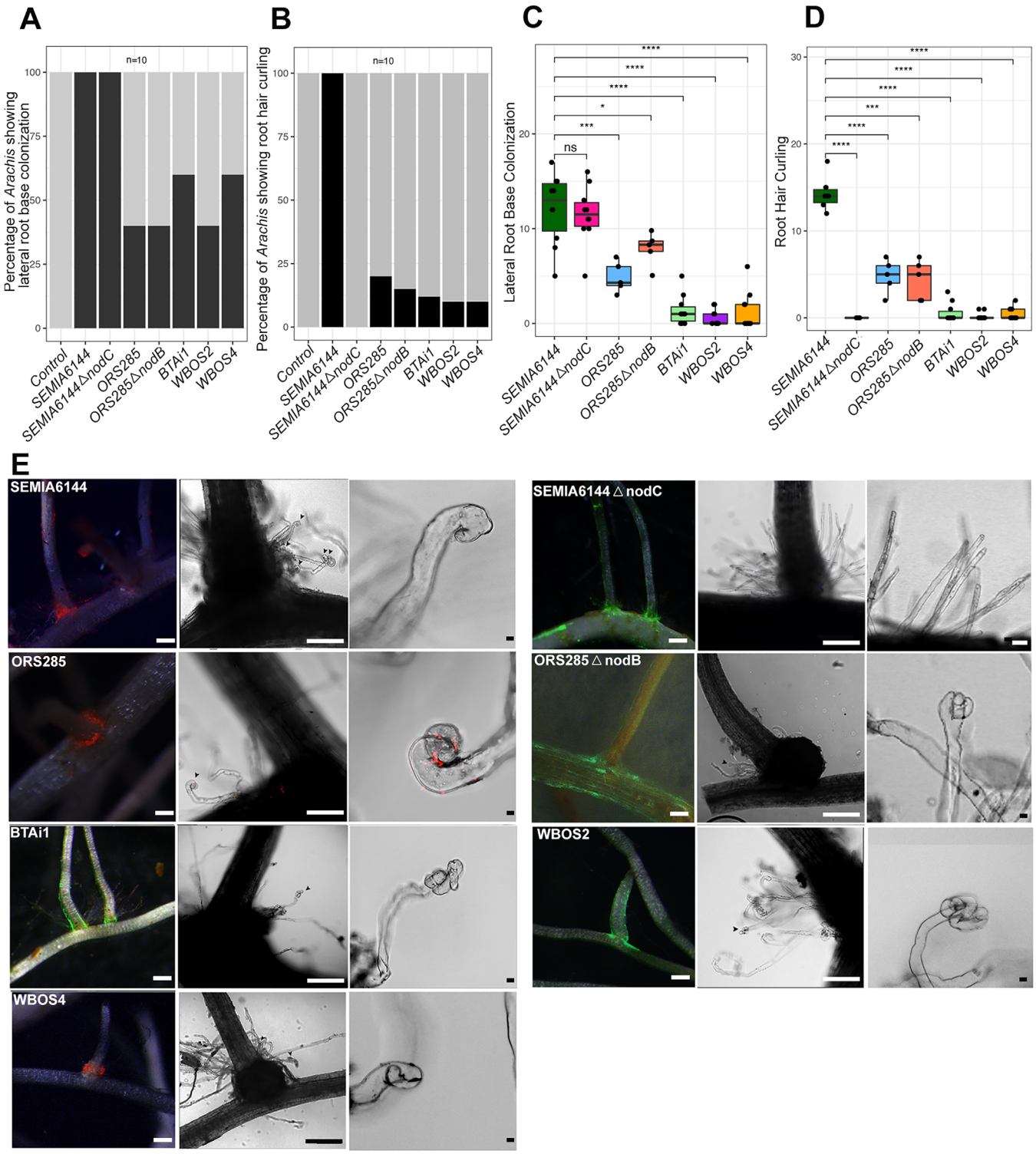

Fig. 4. Legend on next page.

was largely restricted to the nodule surface suggesting it to be sanctioned against entering the nodule (Fig. 5D and Fig. S9). Thus, we observed that NF-deficient WBOS2 which successfully nodulate *A. indica* and *Arachis* can work much better in presence of an NF-producing strain, whereas BTAi1 which is a natural symbiont of *A. indica*

and WBOS4 which can only nodulate *Arachis* during single-strain infection are poor competitors under similar conditions. The outcome was further intriguing when we did the co-inoculation with SEMIA6144 and SEMIA6144ΔnodC that failed to generate any nodule during single inoculation (See Fig. 3A and E). However, in all the SEMIA6144ΔnodC-SEMIA6144 co-inoculated plants, there were at least 11 nodules/plant (39%) which were singly occupied by SEMIA6144ΔnodC where the rhizobia matured into spherical bacteroids while almost 20% of the nodules were occupied by SEMIA6144 and the rest were mixed (Fig. 5C and D; Fig. S7; Table S7). In the mixed nodules, SEMIA6144ΔnodC was confined to the extracellular spaces while the WT strain formed proper spherical bacteroids. Taken together, these observations clearly indicate that the trans-acting NFs from SEMIA6144 were necessary and sufficient to allow successful nodulation by SEMIA6144ΔnodC although in mixed nodules, the NF-containing SEMIA6144 is preferentially intracellularized.

Discussion

Demonstration of NF-independent symbiosis within *Aeschynomene* legumes of the Dalbergoid clade was a paradigm shift in our understanding of RNS (Giraud *et al*., 2007). Depending on the species, *Aeschynomene* legumes can be either Nod-dependent or independent (Miche *et al*., 2010). *Arachis* is also a 'crack-entry' legume where all its natural symbionts are found to be NF-producing, and there is scattered evidence of this legume being nodulated by NF-deficient *Bradyrhizobium* (Noisangiam *et al*., 2012; Guha *et al*., 2016). This led to the question: Is *Arachis* able to support an NF-independent symbiosis similar to the aeschynomenoid legumes? This study is the first systematic attempt that demonstrates that in addition to the NF-dependent symbiosis, there exists an NF-independent symbiosis in *Arachis*.

RNS can be either NF-dependent or NF-independent where host plants usually support a single mechanism of symbiosis (Madsen *et al*., 2010). *Arachis* seems to utilize both the mechanisms depending upon the nature of the rhizobia. This is similar to what was observed in soybean (*G. max* cv. Enrei) which was nodulated by both *Bradyrhizobium elkanii* USDA61 and its *nodC* mutant (Okazaki *et al*., 2013). The profuse nodulation by the cognate symbiont SEMIA6144 and the observed 'no-nodulation' phenotype by SEMIA6144ΔnodC indicate that SEMIA6144 mediated 'crack-entry' mode of symbiosis in *Arachis* happens via the Nod-dependent mechanism (Fig. 3B and E). This draws parallel to similar observations in wild-type IT legumes such as *Medicago* and *L. japonicus*, which fail to nodulate with strains that have been artificially disrupted to produce NFs (Truchet *et al*., 1991; Karas *et al*., 2005). Interestingly in *L. japonicus*, only the gain of function *snf1* mutants are shown to undertake 'crack-entry' mode of symbiosis in an NF-independent manner (Madsen *et al*., 2010).

While NF-dependence of symbiosis in *Arachis* was highlighted by the absence of nodulation by SEMIA6144ΔnodC as has been previously demonstrated by Ibáñez and Fabra (2011), the NF-independent mechanism of symbiosis was clearly demonstrated by nodulation being unaffected in presence of ORS285ΔnodB (Fig. 3B). Interestingly, ORS285 and ORS285ΔnodB could also nodulate *A. indica* with equal efficiency (Bonaldi *et al*., 2011; Lamouche *et al*., 2019) (Fig. 2B). Thus, the symbiotic behaviour of ORS285 is similar in *Arachis* and *A. indica* though the efficiency of symbiosis was much lower in *Arachis*. The inability of SEMIA6144ΔnodC to nodulate *Arachis* does indicate that NFs are important for a successful interaction between *Arachis* and its cognate microsymbiont. But it also indicates that the absence of NFs does not ensure symbiosis using the NF-independent mechanism. Additional dependencies specifically encoded by ORS285 and the naturally *nod* lacking strains seem to be instrumental factors allowing *Arachis* to undertake symbiosis with them. Also, the NF-independent symbiosis is restricted to specific cultivars and is not as robust as the NF-dependent symbiosis (Fig. 1). Thus, we find

Fig. 4. Lateral root base colonization and root hair curling in *Arachis*.
A, B. Percentage of *Arachis* showing lateral root base colonization (A) and root hair curling (B) infected by the indicated *Bradyrhizobium* strains where the number of plants per strain (*n*) is 10. The black and grey areas per bar represent the percentage of colonized and non-colonized plants respectively. Only plants that were responsive for lateral root base colonization were used for scoring the frequencies of colonization and root hair curling per plant.
C. Box plot showing the frequency of lateral root colonization per plant in *Arachis* by the selected *Bradyrhizobium* strains.
D. Box plot showing the frequency of root hair curling per plant in *Arachis* by the selected *Bradyrhizobium* strains. Each data point represents one independent replicate and each experiment involved 10 replicates per strain. One-way ANOVA was used to assess the significant differences among the groups with *P*-values adjusted by Tukey's Multiple Comparison Test. $P > 0.05$ is considered not significant (n.s), whereas '*', '**','***' and '****' indicate $P \leq 0.05$, $P \leq 0.01$, $P \leq 0.001$ and $P \leq 0.0001$ respectively.
E. Lateral root base colonization and root hair curling within *Arachis* induced by the indicated strains. Microscope images of lateral root bases are represented as bright-field + mCherry/GFP merged image showing annular colonization (left), scale bar – 500 μm; Bright-field confocal image of a single lateral root base showing the root hair curlings indicated by black arrowheads (centre), scale bar – 200 μm; Enlarged view of a single root hair curl (right), scale bar for SEMIA6144ΔnodC – 40 μm; rest – 20 μm.

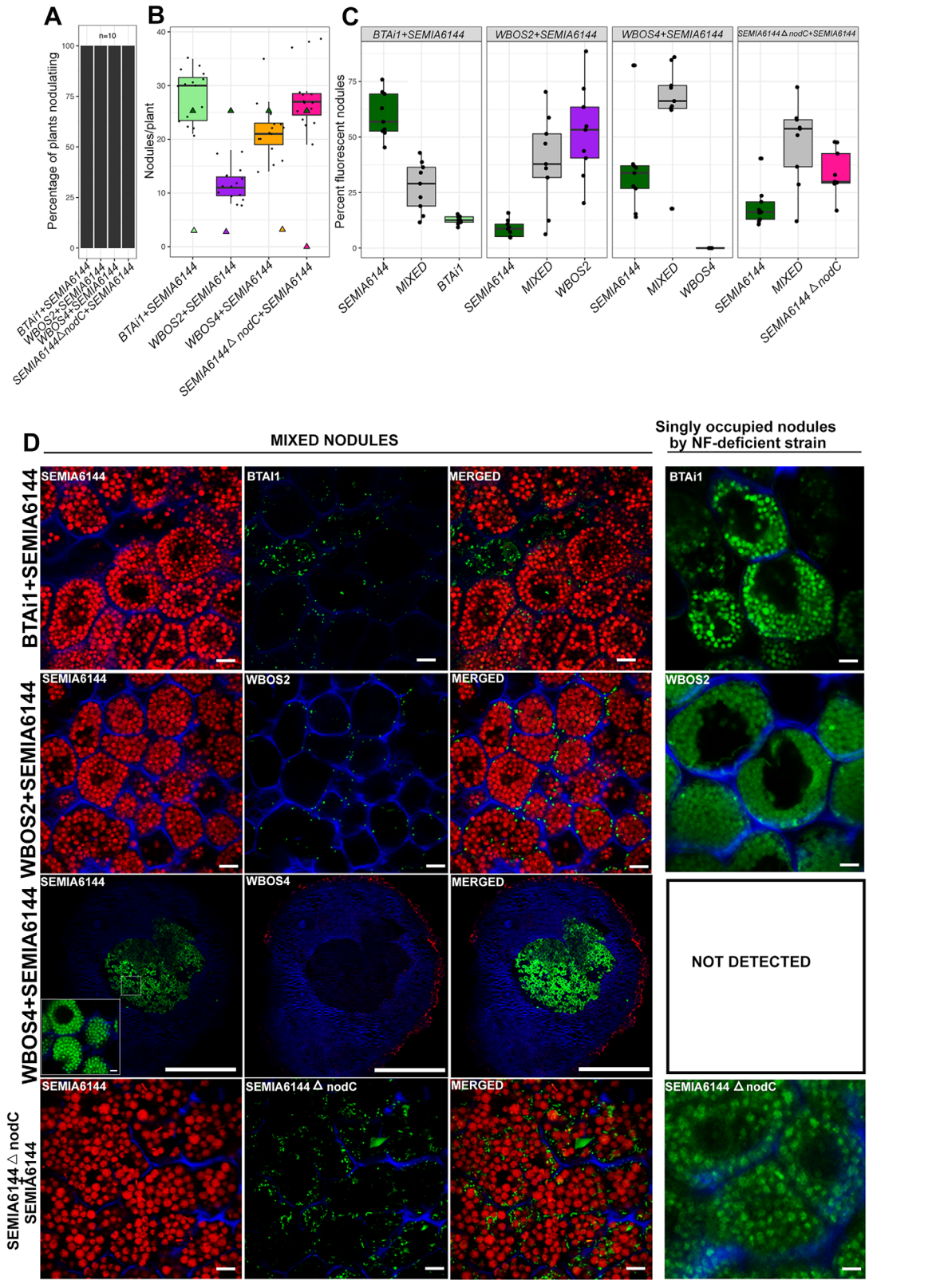

Fig. 5. Legend on next page.

that the choice of the mechanism depends both on the host as well as on the rhizobia encountered. The importance of the rhizobia is further highlighted when we see that for the same host, we get variable nodulation results depending on the incoming rhizobia. While all the NF-deficient strains included in this study successfully nodulated *Arachis*, we obtained a gradient of phenotypes within *A. indica* (Fig. 2B and E). The consistent nodulation by the NF-independent strains within *Arachis* proves that the operative NF-independent symbiosis is less stringent here in comparison to *A. indica* (Fig. 3B). Moreover, the lower degree of nodulation by the NF-deficient strains compared to high nodulation by SEMIA6144 and other *nod*-containing strains, together with the fact that *Arachis* is preferentially nodulated in the fields by *nod*-containing strains indicate the secondary or vestigial nature of the observed NF-independent symbiosis in this legume (Guha *et al*., 2016).

This collection of *Bradyrhizobium* strains could represent excellent systems for comparative genomics studies to enhance our understanding regarding the genetic factors responsible for undertaking NF-independent nodulation.

During the co-infection assays, based on the contribution of the competing NF-deficient strains and SEMIA6144ΔnodC, we were able to classify the inter-strain interactions. It seems as if both SEMIA6144ΔnodC and WBOS2 use SEMIA6144 to gain access into *Arachis*, similar to non-rhizobial *Gammaproteobacter* which have been evidenced to gain access within *Arachis* nodules using SEMIA6144 (Ibáñez *et al*., 2009). Such cases of assisted entry were also seen in *L. japonicus* nodules where *Rhizobium* KAW12 uses the *Mesorhizobium loti (M. loti)* induced IT for accessing the nodules during *M. loti*-KAW12 competition and in *S. rostrata*, where co-infection with a surface polysaccharide mutant and a *nodA* mutant of *Azorhizobium caulinodans* allowed selective nodulation by the *nodA* mutant (D'Haeze *et al*., 1998; Zgadzaj *et al*., 2015). Thus, the presence of SEMIA6144 positively affected the competitiveness of both SEMIA6144ΔnodC and WBOS2. For BTAi1-SEMIA6144 and WBOS4-SEMIA6144, there was substantial suppression of nodulation by the NF-deficient strains (Fig. 5C). Moreover, WBOS4 was completely sanctioned from the nodules, indicating that the presence of SEMIA6144 had a negative effect on these NF-deficient strains (Fig. 5C and D). However, within the mixed nodules, the better-adapted SEMIA6144 was the dominant population, preventing differentiation by the *nod*-lacking strains (Fig. 5D). What triggers this repression, however, is open to further investigation. The mixed nodules could therefore be looked upon as reservoirs meant solely for the persistence of the comparatively lesser efficient NF-deficient strains which would be released in soil following nodule senescence.

In summary, the discovery of NF-independent symbiosis within *Arachis* which already has a well-researched NF-dependent mechanism makes it the only crack-entry legume that is capable of undertaking both. Intriguingly, *Arachis* shares some additional symbiotic features of NF-independent symbiosis with *Aeschynomene*. For example, a cysteine-rich receptor-like kinase which has been implicated in *A. evenia* to be the driver behind the NF-independent symbiosis was significantly upregulated during SEMIA6144-*Arachis* interaction, necessitating further investigation of this receptor in RNS of *Arachis*. (Karmakar *et al*., 2018; Quilbé *et al*., 2021). Also, *Arachis* develops S-morphotype (spherical) bacteroids that are specific for the *Aeschynomene* spp. using an NF-independent symbiotic process, while the E-morphotype (elongated rod) is specific to the *Aeschynomene* spp. using an NF-dependent one (Czernic *et al*., 2015). On the other hand, Nod Factor Hydrolase 1 is absent in *A. evenia*, but its expression in *Arachis* is consistent with the NF-dependent symbiosis with SEMIA6144 (Cai *et al*., 2018; Karmakar *et al*., 2018; Quilbé *et al*., 2021). Type III Secretion System (T3SS) has emerged to be a major determinant in NF-independent symbiosis (Okazaki *et al*., 2016). In *Aeschynomene* legumes, it can either be independent of T3SS as undertaken by photosynthetic bradyrhizobia like BTAi1, or it can be T3SS dependent where ΔT3SS mutants of the non-photosynthetic bradyrhizobia are completely unable to undertake symbiosis, for example as undertaken by ORS3257 (Teulet *et al*., 2019).

Fig. 5. Competition between SEMIA6144 and the NF-deficient strains.
A. Percentage incidence of nodulation among *Arachis* by the selected competition category. The black areas per bar represent the percentage of nodulated plants infected with the indicated strain combination where number of plants per strain (*n*) was 10.
B. Number of nodules per plant produced during competition assays between indicated strain combinations. Triangles indicate nodules produced during single strain inoculations (Dark green: SEMIA6144; Deep-pink: SEMIA6144ΔnodC; Light green: BTAi1; Purple: WBOS2 and Gold: WBOS4) where number of plants per strain (*n*) was 15.
C. Grouped box plots indicating percentage of singly infected fluorescent nodules and mixed nodules (grey) per competition category. Each data point represents one independent replicate where number of plants per competition category (*n*) was 10.
D. Microscopy of mixed nodules and singly occupied nodules by the NF-deficient produced by the indicated competition categories, shown as individual fluorescent fields and GFP/mCherry and Calcofluor stained merged images. Scale bar for WBOS4 + SEMIA6144 – 200 μm; rest – 40 μm.

Similarly, in *G. max*, crack-entry mediated NF-independent symbiosis by nonphotosynthetic bradyrhizobia USDA61 requires an absolute involvement of T3SS (Okazaki *et al*., 2013; Ratu *et al*., 2021). In analogy to these findings, the T3SS-independent mechanism appears to be functional in *Arachis* since photosynthetic bradyrhizobia BTAi1 successfully nodulates it. However, it remains to be understood how T3SS might affect the NF-dependent and NF-independent symbiosis in various cultivars of *Arachis*. Further investigations in *Arachis* might highlight the steps for the evolution of NF as well as T3SS dependence of RNS.

Experimental procedures

Bacterial strains and growth conditions. The bacterial strains and plasmids used in the study are listed in Table S2. *Bradyrhizobium* sp. SEMIA6144 was provided by Dr. Adriana Fabra and *Bradyrhizobium* sp. SEMIA6144ΔnodC was provided by Dr. Fernando Ibáñez, both from CONCINET-UNRC, Rio Cuarto, Argentina. *Bradyrhizobium* sp. BTAi1, ORS285 and ORS285ΔnodB were provided by Dr. Eric Giraud of LSTM (Laboratory of Tropical and Mediterranean Symbioses), Montpellier, France. The pUC18-Tn7T-mini-aad9 plasmid, the GFP and mCherry clusters were kindly provided by Prof. Philip. S. Poole and Dr. Beatrice Jorrín, Department of Plant Sciences, University of Oxford. The WBOS strains were included from a previous study (Guha *et al*., 2016). *Escherichia coli* strains were grown at 37°C in Luria–Bertani medium with antibiotics: ampicillin (100 μg ml^{-1}), kanamycin (20 μg ml^{-1}), spectinomycin (100 μg ml^{-1}) or gentamicin (10 μg ml^{-1}). Unlabelled *Bradyrhizobium* strains were grown in Arabinose-Gluconate (AG) media at 28°C. SEMIA6144ΔnodC was grown in AG media having kanamycin (50 μg ml^{-1}). The labelled bradyrhizobial strains were grown in AG media fortified with 200 μg ml^{-1} spectinomycin and for labelled SEMIA6144ΔnodC, 200 μg ml^{-1} spectinomycin and 50 μg ml^{-1} kanamycin.

Plant sterilization, growth and bacterial infection. Aeschynomene indica seeds were obtained from Dr. Fabienne Cartieaux of LSTM (Laboratory of Tropical and Mediterranean Symbioses), Montpellier, France. Surface sterilization of *A. indica* seeds was done according to Bonaldi *et al*. (2010) followed by gentle rocking in water for 5 h. After abundant washing, the seeds were incubated overnight in sterile water at 4°C. They were transferred onto sterile 0.8% water agar plates and germinated upside down overnight at 28°C in the dark. One day old seedlings were aseptically transferred to sterile vermiculite (Soilrite, Keltech Energies). Two days old plants were used for infection.

Arachis cultivars JL24 (ICRISAT, Hyderabad), ICGV9114 (ICRISAT, Hyderabad), JL501 (Oilseed Research Station, Jalgaon), and locally cultivated Lal Badam (Guha *et al*., 2016) were used in this study. Seeds were surface-sterilized following Sinharoy *et al*. (2009), germinated on sterile moist filter paper overnight at 28°C in dark. One day old seedlings were aseptically transferred to sterile vermiculite. Seven days old plants were used for infection. Both the plants were maintained at 28°C under 16 h/8 h day–night cycle.

The bacterial strains were grown till the early stationary phase (OD_{600}–0.5) in AG broths, the colony forming units was adjusted to 10^6 cells ml^{-1} and 1 ml of this was used to inoculate each plant. For all nodulating strains, only nodulated plants were used for quantification of nodules/plant, plant dry weight and acetylene reduction assay.

Bacterial genetic manipulations and plasmid construction. All PCRs were performed using GoTaq® DNA Polymerase (Promega) using primers listed in Table S2. The plasmids pUC18T-mini-Tn7T-aad9-mCherry and pUC18T-mini-Tn7T-aad9-GFP were constructed by cloning the sfGFP and mCherry cassettes into the BamH1-Pst1 sites of pUC19-mini-Tn7T-aad9 plasmid, using In-Fusion HD Cloning Kit (Clontech) using the primers BamH1-tag-forward/Pst1-tag-reverse. All plasmids were verified by restriction digestion and DNA sequencing. The plasmids were transferred into the bradyrhizobia by tetra-parental mating with pRK2013 and pTNS3 (Choi *et al*., 2006).

Tn7 site of insertion detection. To confirm the insertion of the sfGFP and mCherry cassettes within the strains, we undertook a PCR-based approach, using suitable primer pairs spanning the bradyrhizobial *glmS* gene, and the *aad9* gene of the Tn7 cluster, encoding spectinomycin cassette using the primer pairs $glmS\text{-}_{down}/aad9\text{-}_{rev}$. The resulting amplicons were cloned with pGEMT-Easy vectors (Promega) and subsequently sequenced. Multiple sequence alignment of the clones with the region downstream to the *glmS* in the labelled strains indicated the point of Tn7 insertion.

Acetylene reduction assay. Aeschynomene indica and *Arachis* infected with the selected strains were harvested at 30 dpi. The plants were placed in 250 ml Schott bottles (the true volume being 320 ml) along with a moistened filter paper. 2% of the headspace atmosphere was replaced with acetylene gas (6.4 ml) using a 10 ml syringe fitted with a 22–24 gauge needle. After a 25 h interval, 1 ml of the headspace atmosphere was analyzed by gas chromatography with flame ionization, using Clarus 460 Perkin Elmer Gas Chromatograph fitted with a 50 cm Poropak N column at

70.8°C. The oven temperature was maintained at 80°C with flame ionization detector temperature set to 150°C. The flow rate of the nitrogen carrier gas was set at 20 ml min^{-1}. Nitrogen fixation was calculated as the quantity (nmoles) of ethylene produced per hour per plant according to Haskett *et al*. (2021). For each strain, 10 nodulated plants were assayed for nitrogen fixation. 10 uninoculated plants were included as controls for each strain.

Plant growth promotion experiments. Following acetylene reduction assays, the shoots and roots of the plants were separated and left to dry at 70°C for 7 days following which the dry weights of individual plants were measured as the sum of the dry weights of the corresponding shoots and roots. Uninoculated controls were included in the measurements. All measurements were done with sets of 10 plants per strain.

Lateral root base colonization and root hair curling measurements. We grew *Arachis* embryonic axes on Murashige and Skoog agar plates for 7 days. This was done to make the experiment tractable by generating smaller-sized plants having reduced root systems and countable LRBs. Following the emergence of young roots, the plants were transplanted into sterile vermiculite and were then inoculated with the respective strains (10 plants/strain). The observations were initiated at 4 dpi for SEMIA6144 and SEMIA6144ΔnodC infected plants and at 8 dpi for the plants infected with ORS285, ORS285ΔnodB and the NF-deficient strains, due to delayed onset of colonization for the later strains. The root systems were gently washed with sterile Milli-Q water and were observed under stereofluorescent microscope. Only plants that were responsive for LRB colonization were used for scoring the frequencies of colonization and RHC per plant.

Competition experiments. We grew each strain to the early stationary phase (OD_{600}-0.5). We co-inoculated 7 days old seedlings of *Arachis* with 1 ml of dual strain combinations mixed in a 1:1 ratio. The final CFU was adjusted to 10^6 cells ml^{-1}. We inoculated 10 plants per category which were harvested at 30 dpi. At 30 dpi the plants were harvested, the nodules counted and classified as single infected or mixed based on the emitted fluorescence, under stereofluorescent microscope. Nodules which had either GFP or mCherry fluorescence were considered singly infected while those emitting both the signals were considered mixed nodules. Single or dual infection was further confirmed by observing the nodule interiors under confocal microscope and finally, by identifying the infecting rhizobial population by amplification and sequencing of the housekeeping gene, *recA*, according to Guha *et al*. (2016).

Sectioning and microscopy. All sample preparation for microscopy was carried out following Haynes *et al*. (2004). Image acquisition of the fluorescent whole nodules and nodule half-sections was done using a Leica stereo fluorescence microscope M205FA equipped with a Leica DFC310FX digital camera. The nodules were embedded in Shandon Cryomatrix (Thermo scientific) and semi-thin sections (30- to 40-mm-thick) were prepared using a rotary cryomicrotome CM1850 (Leica Microsystems). The sections were then stained with Calcofluor (Life Technologies) and observed under Leica TCS SP5 II confocal microscope with filters for GFP (excitation 488 nm and emission 509 nm) and mCherry (excitation 587 nm and emission 610 nm). All digital micrographs were processed using Adobe Photoshop CS6 Extended.

Statistical analyses and data visualization. All statistical analyses were performed using GraphPadPrism8. Data visualization was done using the R packages ggplot2 and ggpubr.

Acknowledgements

This work was supported by (i) Indo-UK Nitrogen Fixation Centre (IUNFC), Department of Biotechnology (DBT), Government of India (DBT-BBSRC, BT/IN/UK-VNC/41/DLN/2015-16 to M.D.G.) (ii) IFCPAR/CEFIPRA (IFC/6303-2) and (iii) J C Bose Fellowship to MDG (JCB/2019/000003). S.G., F.M., M.S. acknowledges IUNFC (BT/IN/UK-VNC/41/DLN/2015-16), DBT(BT/PR23731/BPA/118/344/2017), UGC [No. F16-6(DEC.2016/2017)], Council of Scientific and Industrial Research 09/028 (0874)2012-EMR-I], India, for their fellowships.

Author Contributions

S.G. and M.D.G. planned and designed the research. S.G., F.M. and M.S. performed the nodulation assays and F.M. contributed to the labelling of the strains. S.G. performed the microscopy experiments and the competition experiments. F.I. and A.F. provided the SEMIA6144ΔnodC and the SEMIA6144 strains. S.G. and M.D.G. analyzed the data and wrote the manuscript.

References

Arrighi, J.-F., Cartieaux, F., Brown, S.C., Rodier-Goud, M., Boursot, M., Fardoux, J., *et al*. (2012) Aeschynomene evenia, a model plant for studying the molecular genetics of the nod-independent Rhizobium-legume symbiosis. *Mol Plant-Microbe Interact* **25**: 851–861.

Bonaldi, K., Gargani, D., Prin, Y., Fardoux, J., Gully, D., Nouwen, N., *et al*. (2011) Nodulation of *Aeschynomene afraspera* and *A. indica* by photosynthetic *Bradyrhizobium* sp. strain ORS285: the nod-dependent versus the nod-

independent symbiotic interaction. *Mol Plant-Microbe Interact* **24**: 1359–1371.

Bonaldi, K., Gherbi, H., Franche, C., Bastien, G., Fardoux, J., Barker, D., *et al*. (2010) The nod factor-independent symbiotic signaling pathway: development of agrobacterium rhizogenes-mediated transformation for the legume *Aeschynomene indica*. *Mol Plant-Microbe Interact* **23**: 1537–1544.

Cai, J., Zhang, L.-Y., Liu, W., Tian, Y., Xiong, J.-S., Wang, Y.-H., *et al*. (2018) Role of the nod factor hydrolase MtNFH1 in regulating nod factor levels during Rhizobial infection and in mature nodules of *Medicago truncatula*. *Plant Cell* **30**: 397–414.

Chaintreuil, C., Arrighi, J.F., Giraud, E., Miché, L., Moulin, L., Dreyfus, B., *et al*. (2013) Evolution of symbiosis in the legume genus Aeschynomene. *New Phytol* **200**: 1247–1259.

Chandler, M.R. (1978) Some observations on infection of *Arachis hypogaea* L. by rhizobium. *J Exp Bot* **29**: 749–755.

Choi, K.-H., DeShazer, D., and Schweizer, H.P. (2006) mini-Tn7 insertion in bacteria with multiple glmS-linked attTn7 sites: example *Burkholderia mallei* ATCC 23344. *Nat Protoc* **1**: 162–169.

Choi, K.H., Gaynor, J.B., White, K.G., Lopez, C., Bosio, C. M., Karkhoff-Schweizer, R.A.R., and Schweizer, H.P. (2005) A Tn7-based broad-range bacterial cloning and expression system. *Nat Methods* **2**: 443–448.

Czernic, P., Gully, D., Cartieaux, F., Moulin, L., Guefrachi, I., Patrel, D., *et al*. (2015) Convergent evolution of endosymbiont differentiation in Dalbergioid and inverted repeat-lacking clade legumes mediated by nodule-specific cysteine-rich peptides. *Plant Physiol* **169**: 1254–1265.

D'Haeze, W., Gao, M., De Rycke, R., Van Montagu, M., Engler, G., and Holsters, M. (1998) Roles for azorhizobial nod factors and surface polysaccharides in intercellular invasion and nodule penetration, respectively. *Mol Plant Microbe Interact* **11**: 999–1008. https://apsjournals.apsnet.org/doi/10.1094/MPMI.1998.11.10.999

Giraud, E., Moulin, L., Vallenet, D., Barbe, V., Cytryn, E., Avarre, J.C., *et al*. (2007) Legumes symbioses: absence of nod genes in photosynthetic bradyrhizobia. *Science* **316**: 1307–1312.

Goormachtig, S., Capoen, W., James, E.K., and Holsters, M. (2004) Switch from intracellular to intercellular invasion during water stress-tolerant legume nodulation. *Proc Natl Acad Sci U S A* **101**: 6303–6308.

Guha, S., Sarkar, M., Ganguly, P., Uddin, M.R., Mandal, S., and DasGupta, M. (2016) Segregation of nod-containing and nod-deficient bradyrhizobia as endosymbionts of Arachis hypogaea and as endophytes of Oryza sativa in intercropped fields of Bengal basin, India. *Environ Microbiol* **18**: 2575–2590.

Haskett, T.L., Knights, H.E., Jorrin, B., Mendes, M.D., and Poole, P.S. (2021) A simple in situ assay to assess plant-associative bacterial nitrogenase activity. *Front Microbiol* **12**: 690439.

Haynes, J.G., Czymmek, K.J., Carlson, C.A., Veereshlingam, H., Dickstein, R., and Sherrier, D.J. (2004) Rapid analysis of legume root nodule development using confocal microscopy. *New Phytol* **163**: 661–668.

Ibáñez, F., Angelini, J., Taurian, T., Tonelli, M.L., and Fabra, A. (2009) Endophytic occupation of peanut root nodules by opportunistic Gammaproteobacteria. *Syst Appl Microbiol* **32**: 49–55.

Ibáñez, F., and Fabra, A. (2011) Rhizobial nod factors are required for cortical cell division in the nodule morphogenetic programme of the Aeschynomeneae legume Arachis. *Plant Biol* **13**: 794–800.

Jaiswal, S.K., Mohammed, M., Ibny, F.Y.I., and Dakora, F.D. (2021) Rhizobia as a source of plant growth-promoting molecules: potential applications and possible operational mechanisms. *Front Sustain Food Syst* **4**: 619676. https://www.frontiersin.org/articles/10.3389/fsufs.2020.619676/full

Karas, B., Murray, J., Gorzelak, M., Smith, A., Sato, S., Tabata, S., and Szczyglowski, K. (2005) Invasion of Lotus japonicus root hairless 1 by *Mesorhizobium loti* involves the nodulation factor-dependent induction of root hairs. *Plant Physiol* **137**: 1331–1344.

Karmakar, K., Kundu, A., Rizvi, A.Z., Dubois, E., Severac, D., Czernic, P., *et al*. (2018) Transcriptomic analysis with the progress of symbiosis in 'crack-entry' legume *Arachis hypogaea* highlights its contrast with 'infection thread' adapted legumes. *Mol Plant-Microbe Interact* **32**: 271–285. https://apsjournals.apsnet.org/doi/10.1094/MPMI-06-18-0174-R

Lamouche, F., Bonadé-Bottino, N., Mergaert, P., and Alunni, B. (2019) Symbiotic efficiency of spherical and elongated Bacteroids in the Aeschynomene-Bradyrhizobium Symbiosis. *Front Plant Sci* **10**: 377.

Lavin, M., Pennington, R.T., Klitgaard, B.B., Sprent, J.I., De Lima, H.C., and Gasson, P.E. (2001) The dalbergioid legumes (fabaceae): delimitation of a pantropical monophyletic clade. *Am J Bot* **88**: 503–533.

Lehman, S.S., Mladinich, K.M., Boonyakanog, A., Mima, T., Karkhoff-Schweizer, R.R., and Schweizer, H.P. (2016) Versatile nourseothricin and streptomycin/spectinomycin resistance gene cassettes and their use in chromosome integration vectors. *J Microbiol Methods* **129**: 8–13.

Madsen, L.H., Tirichine, L., Jurkiewicz, A., Sullivan, J.T., Heckmann, A.B., Bek, A.S., *et al*. (2010) The molecular network governing nodule organogenesis and infection in the model legume Lotus japonicus. *Nat Commun* **1**: 10.

Miche, L., Moulin, L., Chaintreuil, C., Contreras-Jimenez, J. L., Munive-Hernandez, J.-A., Del Carmen Villegas-Hernandez, M., *et al*. (2010) Diversity analyses of Aeschynomene symbionts in tropical Africa and Central America reveal that nod-independent stem nodulation is not restricted to photosynthetic bradyrhizobia. *Environ Microbiol* **12**: 2152–2164.

Noisangiam, R., Teamtisong, K., Tittabutr, P., Boonkerd, N., Toshiki, U., Minamisawa, K., and Teaumroong, N. (2012) Genetic diversity, symbiotic evolution, and proposed infection process of bradyrhizobium strains isolated from root nodules of *Aeschynomene americana* L. in Thailand. *Appl Environ Microbiol* **78**: 6236–6250.

Okazaki, S., Kaneko, T., Sato, S., and Saeki, K. (2013) Hijacking of leguminous nodulation signaling by the rhizobial type III secretion system. *Proc Natl Acad Sci U S A* **110**: 17131–17136.

Okazaki, S., Tittabutr, P., Teulet, A., Thouin, J., Fardoux, J., Chaintreuil, C., *et al*. (2016) Rhizobium-legume symbiosis

in the absence of nod factors: two possible scenarios with or without the T3SS. *ISME J* **10**: 34–74.
Okubo, T., Fukushima, S., and Minamisawa, K. (2012) Evolution of bradyrhizobium-aeschynomene mutualism: living testimony of the ancient world or highly evolved state? *Plant Cell Physiol* **10**: 64–74.
Oldroyd, G.E.D. (2013) Speak, friend, and enter: signalling systems that promote beneficial symbiotic associations in plants. *Nat Rev Microbiol* **11**: 252–263.
Oldroyd, G.E.D., Murray, J.D., Poole, P.S., and Downie, J.A. (2011) The rules of engagement in the legume-rhizobial symbiosis. *Annu Rev Genet* **45**: 119–144.
Quilbé, J., Lamy, L., Brottier, L., Leleux, P., Fardoux, J., Rivallan, R., *et al*. (2021) Genetics of nodulation in Aeschynomene evenia uncovers mechanisms of the rhizobium–legume symbiosis. *Nat Commun* **12**: 829.
Ratu, S.T.N., Teulet, A., Miwa, H., Masuda, S., Nguyen, H. P., Yasuda, M., *et al*. (2021) Rhizobia use a pathogenic-like effector to hijack leguminous nodulation signalling. *Sci Rep* **11**: 2034.
Sinharoy, S., Saha, S., Chaudhury, S.R., and DasGupta, M. (2009) Transformed hairy roots of *Arachis hypogea*: a tool for studying root nodule Symbiosis in a non–infection thread legume of the Aeschynomeneae tribe. *Mol Plant-Microbe Interact* **22**: 132–142. https://apsjournals.apsnet.org/doi/pdf/10.1094/MPMI-22-2-0132
Sprent, J.I. (2007) Evolving ideas of legume evolution and diversity: a taxonomic perspective on the occurrence of nodulation: Tansley review. *New Phytol* **174**: 11–25.
Teulet, A., Busset, N., Fardoux, J., Gully, D., Chaintreuil, C., Cartieaux, F., *et al*. (2019) The rhizobial type III effector ErnA confers the ability to form nodules in legumes. *Proc Natl Acad Sci U S A* **116**: 21758–21768.
Truchet, G., Roche, P., Lerouge, P., Vasse, J., Camut, S., de Billy, F., *et al*. (1991) Sulphated lipo-oligosaccharide signals of rhizobium meliloti elicit root nodule organogenesis in alfalfa. *Nature* **351**: 670–673. https://www.nature.com/articles/351670a0
Zgadzaj, R., James, E.K., Kelly, S., Kawaharada, Y., de Jonge, N., Jensen, D.B., *et al*. (2015) A legume genetic framework controls infection of nodules by symbiotic and endophytic bacteria. *PLoS Genet* **11**: e1005280.

Supporting Information

Additional Supporting Information may be found in the online version of this article at the publisher's web-site:

Fig. S1. Labelling of *Bradyrhizobium* via Tn7 transposition (A) Map representing the sfGFP and mCherry cassettes along with the spectinomycin encoding gene *aad9*, bounded by Tn7L and Tn7R which indicate the left and right extremities of the insertion clusters, marked with a crimson line, integrated downstream to the *glmS* gene of bradyrhizobial genomes. The black arrows marked '$glmS_{down}$' and '$aad9_{rev}$' represent the primer positions used for identifying the point of Tn7 insertion. (B) Comparative DNA gel images showing the absence and presence of a 1.5 kb amplicon corresponding to the PCR against the primer pair $glmS_{down}$-$aad9_{rev}$ in the unlabelled and labelled *Bradyrhizobium*. Positive PCR indicates the integration of the Tn7 cluster within the selected strains. (C) Nucleotide sequence alignment showing the region downstream to the *glmS* gene (shaded in ash) of the labelled *Bradyrhizobium* strains. The Tn7 point of insertion has been marked with a grey '*' into which the clusters (marked with crimson line) integrate. The intervening 25 base pair (bp) distance is shown. (D) Confocal images of free-living *Bradyrhizobium* cells fluorescently labelled via Tn7 transposition. Scale Bar-1 μm

Fig. S2. Plant growth promotion in *A. indica* by *Bradyrhizobium* sp. strains Comparison of growth of *A. indica* plants (aerial part), non-inoculated control (Control) or inoculated with the indicated *Bradyrhizobium* strains at 30 dpi.

Fig. S3. Fluorescent nodules induced in *Arachis* by indicated *Bradyrhizobium* sp. strains. Scale bar for SEMIA6144:1 mm; Scale bar for rest:500 μm .

Fig. S4. Plant growth promotion in *Arachis* by *Bradyrhizobium* sp. strains. Comparison of growth of *Arachis* plants (aerial part), non-inoculated control (Control) or inoculated with the indicated *Bradyrhizobium* strains at 30 dpi.

Fig. S5. Root hair branching in *Arachis* infected by *Bradyrhizobium* sp. strains. Scale bar- 40 μm .

Fig. S6. Confocal image of SEMIA6144 induced root hair curl showing occasional bacterial entrapment within the curled root hair. Scale bar- 200 μm (left) and 40 μm (right).

Fig. S7. Stereomicroscope images of the different types of nodules produced during competition assays. Stereofluorescent images of mixed nodules and singly occupied nodules by the NF-deficient produced by the indicated competition categories, shown as individual fluorescent fields and GFP/mCherry and Calcofluor stained merged images. Scale bar- 500 μm

Fig. S8. Mixed nodule produced during BTAi1 + SEMIA6144 competition assay (A) Entire nodule section showing dominant BTAi1 and restricted SEMIA6144 population. Scale bar-200 μm (B) Enlarged view of infection zone of the mixed nodule showing spherical bacteroids of SEMIA6144 co-existing with BTAi1. Scale bar-40 μm

Fig. S9. Colonization of WBOS4 during WBOS4 + SEMIA6144 competition (A) Entire nodule section showing GFP-labelled SEMIA6144 induced infection zone while mCherry labelled WBOS4 is restricted to the outer epidermis. (B) and (C) represent progressive magnified images clearly indicating WBOS4 to be stuck to the outer epidermis of the nodule. Scale bar for (A)-200 μm; (B)-40 μm; (C)-10 μm

Table S1. Antibiotic sensitivities of the *Bradyrhizobium* strains used in the study

Table S2. List of strains, plasmids and primers used in the study

Table S3. Nodulation efficiencies of the selected strains in *A. indica*

Table S4. Nodulation efficiencies of the selected strains in *Arachis*.

Table S5. Lateral root base colonization and root hair curling counts in *Arachis* induced by the selected strains

Table S6. Nodulation efficiencies during competition assays in *Arachis*

Table S7. Singly occupied nodules and mixed nodules formed by each competition category